

## Structure and Properties of the Thorium Vanadyl Tellurate, $\text{Th}(\text{VO}_2)_2(\text{TeO}_6)(\text{H}_2\text{O})_2$

Tyler A. Sullens and Thomas E. Albrecht-Schmitt\*

Department of Chemistry and Biochemistry, Auburn University, Auburn, Alabama 36849

Received December 10, 2004

The hydrothermal reaction of  $\text{Th}(\text{NO}_3)_4 \cdot x\text{H}_2\text{O}$  with  $\text{V}_2\text{O}_5$  and  $\text{H}_6\text{TeO}_6$  at 200 °C under autogenously generated pressure results in the formation of  $\text{Th}(\text{VO}_2)_2(\text{TeO}_6)(\text{H}_2\text{O})_2$  as a pure phase. The single-crystal X-ray data indicate that  $\text{Th}(\text{VO}_2)_2(\text{TeO}_6)(\text{H}_2\text{O})_2$  possesses a three-dimensional structure constructed from  $\text{ThO}_9$  tricapped trigonal prisms,  $\text{VO}_5$  distorted square pyramids,  $\text{VO}_4$  distorted tetrahedra, and  $\text{TeO}_6$  distorted octahedra. Both of the vanadium polyhedra contain  $\text{VO}_2^+$  vanadyl units with two short  $\text{V}=\text{O}$  bond distances. The tellurate octahedron is tetragonally distorted and utilizes all of its oxygen atoms to bond to adjacent metal centers, sharing edges with  $\text{ThO}_9$  and  $\text{VO}_5$  units, and corners with two  $\text{ThO}_9$ , one  $\text{VO}_5$ , and two  $\text{VO}_4$  polyhedra. Crystallographic data:  $\text{Th}(\text{VO}_2)_2(\text{TeO}_6)(\text{H}_2\text{O})_2$ , orthorhombic, space group *Pbca*,  $a = 12.6921(7)$ ,  $b = 11.5593(7)$ ,  $c = 13.0950(8)$  Å,  $Z = 8$  ( $T = 193$  K). The UV–vis diffuse reflectance spectrum of  $\text{Th}(\text{VO}_2)_2(\text{TeO}_6)(\text{H}_2\text{O})_2$  shows vanadyl-based charge-transfer absorption features.  $\text{Th}(\text{VO}_2)_2(\text{TeO}_6)(\text{H}_2\text{O})_2$  decomposes primarily to  $\text{Th}(\text{VO}_3)_4$  when heated at 600 °C in air.

### Introduction

Periodate,  $\text{IO}_6^{5-}$ , and tellurate,  $\text{TeO}_6^{6-}$ , have played pivotal roles in the isolation of transition metal complexes with unusually high oxidation states.<sup>1</sup> The tellurate anion has been shown to stabilize Ru(VI) and Os(VI) in  $\text{Na}_6[\text{RuO}_2\{\text{TeO}_4(\text{OH})_2\}_2] \cdot 16\text{H}_2\text{O}$ <sup>2</sup> and  $\text{Rb}_2\text{Na}_4[\text{OsO}_2\{\text{TeO}_4(\text{OH})_2\}_2] \cdot 18\text{H}_2\text{O}$ ,<sup>3</sup> Pd(IV) in  $\text{Na}_8\text{K}_2\text{H}_4[\text{Pd}_2\text{Te}_4\text{O}_{24}\text{H}_2] \cdot 20\text{H}_2\text{O}$ ,<sup>4</sup> Cu(III) in  $\text{Na}_5[\text{Cu}\{\text{TeO}_4(\text{OH})_2\}_2] \cdot 16\text{H}_2\text{O}$ ,<sup>5</sup> Ag(III) in  $\text{Na}_5[\text{Ag}\{\text{TeO}_4(\text{OH})_2\}_2] \cdot 16\text{H}_2\text{O}$ ,<sup>2</sup> and Au(III) in  $\text{Na}_5[\text{Au}\{\text{TeO}_4(\text{OH})_2\}_2] \cdot 16\text{H}_2\text{O}$ .<sup>6</sup> By comparison, well-characterized examples of actinide periodate and tellurate complexes are sparse.<sup>1</sup> There are only two known uranyl periodates,  $\text{A}[(\text{UO}_2)_3(\text{HIO}_6)_2(\text{OH})(\text{O})(\text{H}_2\text{O})] \cdot 1.5\text{H}_2\text{O}$  ( $\text{A} = \text{Li}–\text{Cs}, \text{Ag}$ )<sup>7</sup> and  $\text{K}_2[(\text{UO}_2)_2(\text{VO})_2(\text{IO}_6)_2\text{O}] \cdot \text{H}_2\text{O}$ ,<sup>8</sup> both of which possess polar open-framework structures, and no known examples of actinide tellurate compounds.<sup>1</sup> In addition to offering the possibility

of stabilizing high oxidation states in actinides, periodate and tellurate provide the opportunity to build structures with three-dimensional connectivity<sup>9,10</sup> because of their approximately octahedral geometries and their ability to bind a large number of metal centers.<sup>1,5,6</sup>

In an effort to understand the structural chemistry of tellurate with actinides, we have investigated the reaction of Th(IV) salts with a variety of tellurate sources primarily under mild hydrothermal conditions. These studies have resulted in the isolation of the mixed-metal thorium vanadyl tellurate,  $\text{Th}(\text{VO}_2)_2(\text{TeO}_6)(\text{H}_2\text{O})_2$ , which represents the first actinide tellurate whose constitution is unambiguously defined. This compound also provides information on vanadyl tellurate coordination, which is also absent from the literature. Herein, we report the structure and properties of  $\text{Th}(\text{VO}_2)_2(\text{TeO}_6)(\text{H}_2\text{O})_2$ .

### Experimental Section

**Syntheses.**  $\text{Th}(\text{NO}_3)_4 \cdot x\text{H}_2\text{O}$  (99%, Alfa-Aesar),  $\text{V}_2\text{O}_5$  (99.9%, Alfa-Aesar), and  $\text{H}_6\text{TeO}_6$  (99.5%, Alfa-Aesar) were used as received. Reactions were performed in PTFE-lined Parr 4749 autoclaves. Distilled and Millipore filtered water with a resistance of 18.2 MΩ cm was used in all reactions. Standard precautions were performed for handling radioactive materials during work with

\* Author to whom correspondence should be addressed. E-mail: albretht@auburn.edu.

- (1) Levason, W. *Coord. Chem. Rev.* **1997**, *161*, 33.
- (2) Hector, A. L.; Hill, N. J.; Levason, W.; Webster, M. Z. *Anorg. Allg. Chem.* **2002**, *628*, 815.
- (3) Levason, W.; Oldroyd, R. D.; Webster, M. *J. Chem. Soc., Dalton Trans.* **1994**, *20*, 2983.
- (4) Levason, W.; Spicer, M. D.; Webster, M. *Inorg. Chem.* **1991**, *30*, 967.
- (5) Levason, W.; Spicer, M. D.; Webster, M. *J. Chem. Soc., Dalton Trans.* **1988**, *5*, 1377.
- (6) Levason, W.; Webster, M. *Acta Crystallogr.* **1998**, *C54*, 1729.
- (7) Sullens, T. A.; Jensen, R. A.; Shvareva, T. Y.; Albrecht-Schmitt, T. E. *J. Am. Chem. Soc.* **2004**, *126*, 2676.
- (8) Sykora, R. E.; Albrecht-Schmitt, T. E. *Inorg. Chem.* **2003**, *42*, 2179.

(9) Ok, K. M.; Halasyamani, P. S. *Solid State Sci.* **2002**, *4*, 793.

(10) Yu, R.; Ok, K. M.; Halasyamani, P. S. *J. Chem. Soc., Dalton Trans.* **2004**, *3*, 392.

$\text{Th}(\text{NO}_3)_4 \cdot x\text{H}_2\text{O}$  and  $\text{Th}(\text{VO}_2)_2(\text{TeO}_6)(\text{H}_2\text{O})_2$ . Semiquantitative SEM/EDX analyses were performed using a JEOL 840/Link Isis instrument. Th, V, and Te percentages were calibrated against standards. The IR spectrum was collected on a Nicolet 5PC FT-IR spectrometer from a KBr pellet.

**$\text{Th}(\text{VO}_2)_2(\text{TeO}_6)(\text{H}_2\text{O})_2$ .**  $\text{Th}(\text{NO}_3)_4 \cdot x\text{H}_2\text{O}$  (0.2812 g, 0.5857 mmol),  $\text{V}_2\text{O}_5$  (0.1061 g, 0.5834 mmol), and  $\text{H}_6\text{TeO}_6$  (0.1128 g, 0.4912 mmol) were loaded into a 23-mL PTFE-lined autoclave. Water (1 mL) was then added to the reaction mixture. The autoclave was sealed and placed into a box furnace and heated to 200 °C. After 6 d, the reaction was cooled at a rate of 9 °C/h to 23 °C. The product mixture consisted of clusters of acicular yellow crystals in a green mother liquor. The mother liquor was decanted, and the crystals were then washed with water and methanol and allowed to dry. Yield, 299 mg (79% based on Th). Phase purity was confirmed by powder X-ray diffraction measurements. The measured powder pattern was compared to a pattern calculated from single-crystal X-ray data using ATOMS (v. 5, Shape Software). No extraneous diffraction peaks were observed. IR (KBr,  $\text{cm}^{-1}$ ): 1613 ( $\delta$ ,  $\text{H}_2\text{O}$ , w), 979 ( $\nu$ ,  $\text{VO}_2^+$ , s), 964 ( $\nu$ ,  $\text{VO}_2^+$ , s), 955 ( $\nu$ ,  $\text{VO}_2^+$ , s), 930 ( $\nu$ ,  $\text{VO}_2^+$ , s), ( $\nu$ , V—O, Te—O, Th—O) 862 (s), 843 (m), 821 (w), 796 (w, sh), 760 (s), 724 (w, sh), 695 (s). EDX measurements show a Th:V:Te ratio of approximately 1(27%):2(47%):1(26%).

**Thermal Analysis.** Thermal data for  $\text{Th}(\text{VO}_2)_2(\text{TeO}_6)(\text{H}_2\text{O})_2$  were collected using a TA Instruments, model 2920 differential scanning calorimeter (DSC) and a TA Q50 Thermogravimetric Analyzer (TGA). Samples (~20 mg) were encapsulated in aluminum or platinum pans and heated at 10 °C/min from 25 to 600 °C under a nitrogen atmosphere.

**UV–Vis Diffuse Reflectance Spectra.** The diffuse reflectance spectrum of  $\text{Th}(\text{VO}_2)_2(\text{TeO}_6)(\text{H}_2\text{O})_2$  was measured from 1800 to 200 nm using a Shimadzu UV3100 spectrophotometer equipped with an integrating sphere attachment with  $\text{BaSO}_4$  as the standard. The Kubelka–Monk function was used to convert diffuse reflectance data to absorbance spectra.<sup>11</sup>

**X-ray Powder Diffraction Data.** Powder diffraction data were collected using a Rigaku Miniflex powder diffractometer using  $\text{Cu K}\alpha$  ( $\lambda = 1.54056 \text{ \AA}$ ) radiation. Data were compared to patterns from the ICDD database or to those calculated directly from single-crystal data using ATOMS.

**Crystallographic Studies.** A single crystal of  $\text{Th}(\text{VO}_2)_2(\text{TeO}_6)(\text{H}_2\text{O})_2$  was mounted on a glass fiber and aligned on a Bruker SMART APEX CCD X-ray diffractometer. Intensity measurements were performed using graphite monochromated  $\text{Mo K}\alpha$  radiation from a sealed tube and monochromator. SMART (v 5.624) was used for preliminary determination of the cell constants and data collection control. The intensities of reflections of a sphere were collected by a combination of three sets of exposures (frames). Each set had a different  $\phi$  angle for the crystal, and each exposure covered a range of 0.3° in  $\omega$ . A total of 1800 frames were collected with an exposure time per frame of 30 s.

For  $\text{Th}(\text{VO}_2)_2(\text{TeO}_6)(\text{H}_2\text{O})_2$ , determination of integrated intensities and global refinement were performed with the Bruker SAINT (v 6.02) software package using a narrow-frame integration algorithm. A face-indexed analytical absorption correction was initially applied using XPREP, where individual shells of unmerged data were corrected analytically.<sup>12</sup> These files were subsequently treated with a semiempirical absorption correction by SADABS.<sup>13</sup> The program suite SHELXTL (v 6.12) was used for space group

**Table 1.** Crystallographic Data for  $\text{Th}(\text{VO}_2)_2(\text{TeO}_6)(\text{H}_2\text{O})_2$

formula	$\text{Th}(\text{VO}_2)_2(\text{TeO}_6)(\text{H}_2\text{O})_2$
formula mass	657.55
color and habit	yellow needle
crystal system	orthorhombic
space group	<i>Pbca</i> (No. 61)
<i>a</i> (Å)	12.6921(7)
<i>b</i> (Å)	11.5593(7)
<i>c</i> (Å)	13.0950(8)
<i>V</i> (Å <sup>3</sup> )	1921.2(2)
<i>Z</i>	8
<i>T</i> (K)	193
$\lambda$ (Å)	0.71073
maximum $2\theta$ (deg)	56.58
$\rho_{\text{calcd}}$ ( $\text{g cm}^{-3}$ )	4.519
$\mu(\text{Mo K}\alpha)$ ( $\text{cm}^{-1}$ )	203.83
$R(F)$ for $F_o^2 > 2\sigma(F_o^2)^a$	0.0250
$R_w(F_o^2)^b$	0.0622

$$^a R(F) = \sum ||F_o| - |F_c|| / \sum |F_o|. \quad ^b R_w(F_o^2) = [\sum [w(F_o^2 - F_c^2)^2] / \sum wF_o^4]^{1/2}.$$

determination (XPREP), direct methods structure solution (XS), and least-squares refinement (XL).<sup>12</sup> The final refinements included anisotropic displacement parameters for all atoms. Secondary extinction was not noted. Some crystallographic details are given in Table 1. Additional details can be found in the Supporting Information.

## Results and Discussion

**Synthesis.** The challenge in preparing actinide tellurates, and periodates for that matter, is that these anions oxidize water and are reduced by two electrons from Te(VI) or I(VII) to Te(IV) or I(V). Under hydrothermal conditions, these processes occur quite rapidly, which coincidentally is a convenient method for crystallizing tellurite and iodate compounds.<sup>14–16</sup> It was discovered in the course of preparing  $\text{K}_2[(\text{UO}_2)_2(\text{VO}_2)(\text{IO}_6)_2\text{O}] \cdot \text{H}_2\text{O}$ <sup>8</sup> that the presence of  $\text{V}_2\text{O}_5$  inhibits the reduction of periodate. We therefore applied this method to the synthesis of thorium tellurates and found that the reaction of  $\text{Th}(\text{NO}_3)_4 \cdot x\text{H}_2\text{O}$  with  $\text{V}_2\text{O}_5$  and telluric acid results in the isolation of a desired product,  $\text{Th}(\text{VO}_2)_2(\text{TeO}_6)(\text{H}_2\text{O})_2$ , that contains Th(IV), V(V), and Te(VI), in both high yield and purity.

**Structure of  $\text{Th}(\text{VO}_2)_2(\text{TeO}_6)(\text{H}_2\text{O})_2$ .** The structure of  $\text{Th}(\text{VO}_2)_2(\text{TeO}_6)(\text{H}_2\text{O})_2$  is three-dimensional in nature and is constructed from  $\text{ThO}_9$  tricapped trigonal prisms,  $\text{VO}_5$  distorted square pyramids,  $\text{VO}_4$  distorted tetrahedra, and  $\text{TeO}_6$  distorted octahedra. An ORTEP diagram showing these building units is shown in Figure 1. The oxidation states can be assigned in this compound as Th(IV), V(V) at both sites, and Te(VI). The Th—O bond distances range from 2.282(4) to 2.601(5) Å. The  $\text{ThO}_9$  units share one edge with the  $\text{VO}_5$

(11) Wendlandt, W. W.; Hecht, H. G. *Reflectance Spectroscopy*; Interscience Publishers: New York, 1966.

- (12) Sheldrick, G. M. *SHELXTL PC, Version 6.12, An Integrated System for Solving, Refining, and Displaying Crystal Structures from Diffraction Data*; Siemens Analytical X-ray Instruments, Inc.: Madison, WI, 2001.
- (13) Sheldrick, G. M. *SADABS 2001*, Program for absorption correction using SMART CCD based on the method of Blessing; Blessing, R. H. *Acta Crystallogr.* **1995**, *A51*, 33.
- (14) Bean, A. C.; Peper, S. M.; Albrecht-Schmitt, T. E. *Chem. Mater.* **2001**, *13*, 1266.
- (15) Hector, A. L.; Henderson, S. J.; Levason, W.; Webster, M. Z. *Anorg. Allg. Chem.* **2002**, *628*, 198.
- (16) Douglas, P.; Hector, A. L.; Levason, W.; Light, M. E.; Matthews, M. L.; Webster, M. Z. *Anorg. Allg. Chem.* **2004**, *630*, 479.

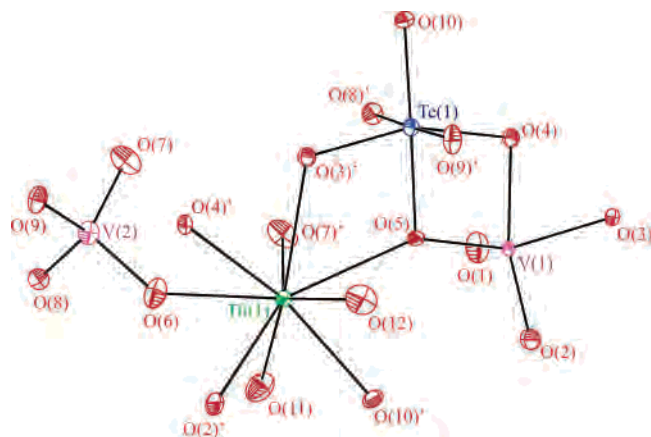


**Figure 1.** A view of the ThO<sub>9</sub> tricapped trigonal prisms, VO<sub>5</sub> distorted square pyramids, VO<sub>4</sub> distorted tetrahedra, and TeO<sub>6</sub> distorted octahedra in Th(VO<sub>2</sub>)<sub>2</sub>(TeO<sub>6</sub>)(H<sub>2</sub>O)<sub>2</sub>. 50% probability ellipsoids are depicted.

**Table 2.** Selected Bond Distances (Å) and Angles (deg) for Th(VO<sub>2</sub>)<sub>2</sub>(TeO<sub>6</sub>)(H<sub>2</sub>O)<sub>2</sub>

Distances (Å)			
Th(1)–O(2)	2.384(4)	V(1)–O(4)	2.044(4)
Th(1)–O(3)	2.479(4)	V(1)–O(5)	1.929(4)
Th(1)–O(4)	2.430(4)	V(2)–O(6)	1.654(5)
Th(1)–O(5)	2.528(4)	V(2)–O(7)	1.654(5)
Th(1)–O(6)	2.455(5)	V(2)–O(8)	1.771(4)
Th(1)–O(7)	2.400(5)	V(2)–O(9)	1.801(4)
Th(1)–O(10)	2.282(4)	Te(1)–O(3)	1.921(4)
Th(1)–O(11)	2.564(5)	Te(1)–O(4)	1.907(4)
Th(1)–O(12)	2.601(5)	Te(1)–O(5)	1.943(4)
V(1)–O(1)	1.628(5)	Te(1)–O(8)	1.948(4)
V(1)–O(2)	1.671(5)	Te(1)–O(9)	1.953(4)
V(1)–O(3)	1.945(4)	Te(1)–O(10)	1.829(4)
Angles (deg)			
O(1)–V(1)–O(2)	106.3(3)	O(6)–V(2)–O(7)	111.2(3)
O(10)–Te(1)–O(4)	101.61(17)	O(3)–Te(1)–O(4)	159.49(17)
O(10)–Te(1)–O(3)	98.90(17)	O(10)–Te(1)–O(5)	178.60(19)
O(4)–Te(1)–O(5)	78.98(17)	O(3)–Te(1)–O(5)	80.51(17)
O(10)–Te(1)–O(8)	88.04(19)	O(4)–Te(1)–O(8)	88.73(17)
O(3)–Te(1)–O(8)	91.61(17)	O(5)–Te(1)–O(8)	90.71(18)
O(10)–Te(1)–O(9)	90.20(19)	O(4)–Te(1)–O(9)	92.84(17)
O(3)–Te(1)–O(9)	87.44(17)	O(5)–Te(1)–O(9)	91.04(18)
O(8)–Te(1)–O(9)	177.84(18)		

polyhedra and a second edge with the TeO<sub>6</sub> octahedra. This unit has six additional corner-sharing interactions: two with the VO<sub>5</sub> distorted square pyramids, two with the VO<sub>4</sub> distorted tetrahedra, and two more with the TeO<sub>6</sub> octahedra. These interactions result in three  $\mu_3$ -O atoms (O(3), O(4), and O(5)) and four  $\mu_2$ -O atoms (O(2), O(6), O(7), and O(10)). The two remaining oxygen atoms (O(11) and O(12)) are concluded to be water molecules on the basis of their long Th–O bond distances of 2.564(5) and 2.601(5) Å, their bond valence sums of 0.34 and 0.31,<sup>17,18</sup> charge balance requirements, and the presence of water stretching and bending modes in the IR spectrum. Selected bond distances and angles are given in Table 2.

There are two crystallographically unique vanadium atoms in Th(VO<sub>2</sub>)<sub>2</sub>(TeO<sub>6</sub>)(H<sub>2</sub>O)<sub>2</sub> in two different coordination environments. V(1) is in a five-coordinate distorted square pyramidal geometry. V(2) meanwhile is found in a distorted tetrahedral environment. Both of the V(V) polyhedra contain a VO<sub>2</sub><sup>+</sup> vanadyl unit with two short V=O bond distances. V(1) has vanadyl oxygen bond lengths of 1.628(5) and

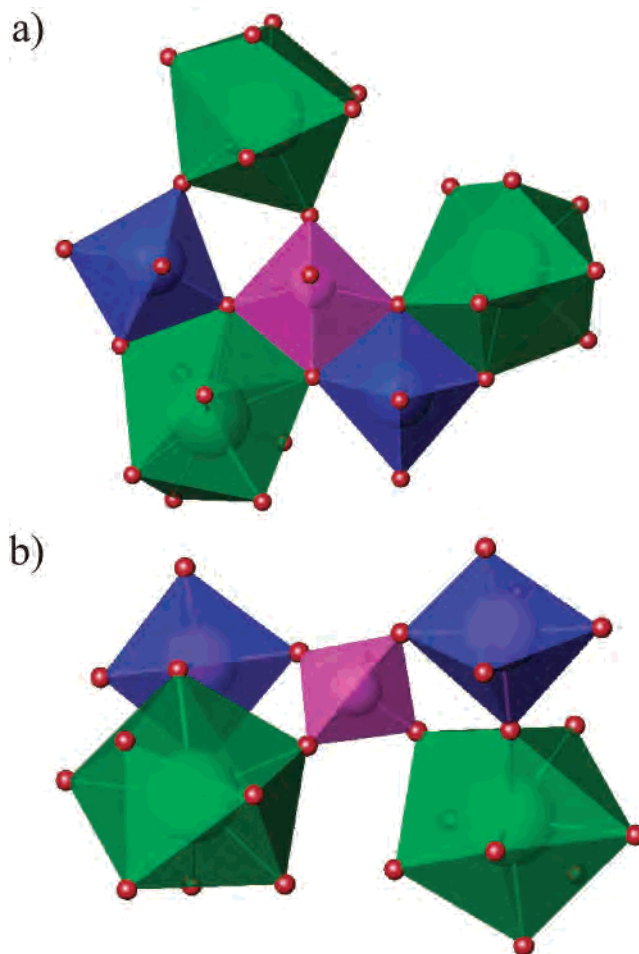


**Figure 2.** (a) A depiction of the interactions between the VO<sub>5</sub> distorted square pyramids and neighboring polyhedra in Th(VO<sub>2</sub>)<sub>2</sub>(TeO<sub>6</sub>)(H<sub>2</sub>O)<sub>2</sub>. Edge-sharing occurs with one ThO<sub>9</sub> unit and one TeO<sub>6</sub> unit. Corner-sharing occurs with two additional ThO<sub>9</sub> tricapped trigonal prisms and one TeO<sub>6</sub> octahedron. (b) The VO<sub>4</sub> units corner-share with two ThO<sub>9</sub> units and two TeO<sub>6</sub> units. Vanadium polyhedra are shown in magenta, thorium in green, and tellurium are in blue.

1.671(5) Å to O(1) and O(2), respectively, and an O(1)–V(1)–O(2) bond angle of 106.3(3)°. The shorter V(1)–O(1) bond distance reflects its terminal nature. The remaining four oxygen atoms in the V(1)O<sub>5</sub> units are bridging. The distortion of the V(1)O<sub>5</sub> unit is evident in the bond angles of the square base of the unit. The O(3)–V(1)–O(4) angle is 74.84(17)°, which is close to that of the adjacent O(4)–V(1)–O(5) angle of 76.02(16)°. An examination of the remaining base angles shows this distortion with O(2)–V(1)–O(3) and O(2)–V(1)–O(5) having bonding angles of 94.97(19)° and 99.47(19)°, respectively. The VO<sub>5</sub> polyhedron contains several interactions with adjacent polyhedra. There are two edge-sharing interactions: one with a ThO<sub>9</sub> unit and a second with a TeO<sub>6</sub> unit, both involving  $\mu_3$ -O(4). The O(3) and O(5) atoms are also  $\mu_3$  because the VO<sub>5</sub> unit utilizes O(3) and O(5) to edge-share or corner-share with either a ThO<sub>9</sub> tricapped trigonal prism or a TeO<sub>6</sub> octahedron. A depiction of these complex combinations is shown in Figure 2a.

The tetrahedral VO<sub>4</sub> units containing V(2) are distorted from ideality. The bond distances observed within the

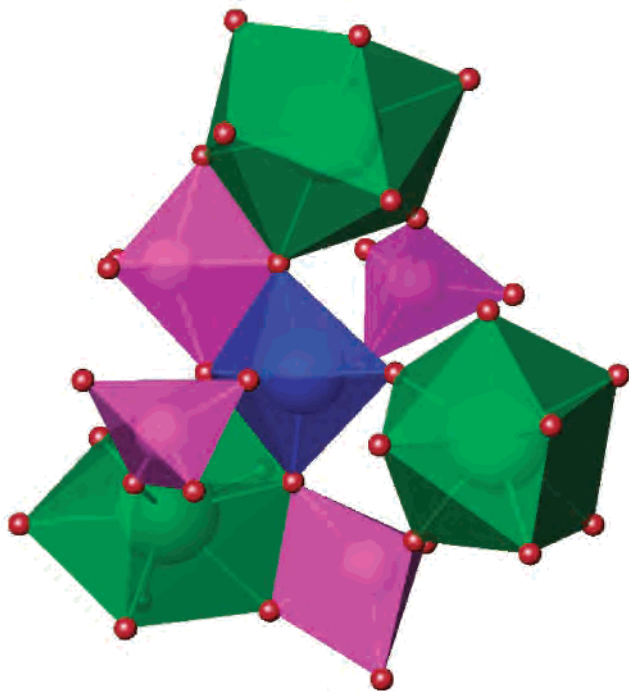


**Figure 3.** An illustration of the bonding for the tellurate,  $\text{TeO}_6^{6-}$ , anion in  $\text{Th}(\text{VO}_2)_2(\text{TeO}_6)(\text{H}_2\text{O})_2$ . All six oxygen atoms are used to bind neighboring metal centers, resulting in two edge-sharing interactions with a  $\text{ThO}_9$  unit and one with a  $\text{VO}_5$  unit. Corner-sharing interactions also occur with one  $\text{ThO}_9$ , one  $\text{VO}_5$ , and two  $\text{VO}_4$  polyhedra. Vanadium polyhedra are shown in magenta, thorium are in green, and tellurium are in blue.

vanadyl unit of  $\text{VO}_4$  tetrahedron are similar to those found within  $\text{VO}_5$  unit with a distance of 1.654(5) Å to both O(6) and O(7), and a bond angle of 111.2(3)°. The remaining V–O bond lengths are V(2)–O(8) at 1.771(4) Å, and V(2)–O(9) at 1.801(4) Å. The bond angles range from 105.3(2)° to 119.2(2)°. The  $\text{VO}_4$  units only corner-share with adjacent polyhedra, leaving all oxygen atoms as bridging: O(6) and O(7) to Th(1) and O(8) and O(9) to Te(1). A view of these interactions is shown in Figure 2b.

The tellurate anions, containing Te(VI), are highly distorted from idealized octahedral symmetry with Te–O bond distances ranging from 1.829(4) to 1.953(4) Å. The distortion is approximately tetragonal in nature and is in the direction of O(10), this being the shortest Te–O bond distance of 1.829(4) Å. The O–Te–O bond angles given in Table 2 also demonstrate the deviation of the tellurate anion from octahedral symmetry. The  $\text{TeO}_6^{6-}$  anion utilizes all of its oxygen atoms to bond to adjacent polyhedra with one edge-sharing interaction with a  $\text{ThO}_9$  unit and another with a  $\text{VO}_5$  unit. Corner-sharing interactions also occur with two  $\text{ThO}_9$ , one  $\text{VO}_5$ , and two  $\text{VO}_4$  polyhedra as shown in Figure 3. These bonds result in three  $\mu_2$ -O atoms (O(3), O(4), and O(5)) as well as three  $\mu_3$ -O atoms (O(8), O(9), and O(10)).

The triad that forms from the  $\text{ThO}_9$ ,  $\text{VO}_5$ , and  $\text{TeO}_6$  through edge-sharing is the essential building block of part of the structure of  $\text{Th}(\text{VO}_2)_2(\text{TeO}_6)(\text{H}_2\text{O})_2$ . These units form a continuum of edge-sharing interactions to create Th–V–Te oxide chains, which extend along the  $b$ -axis as shown in Figure 4a. Corner-sharing interactions between the  $\text{TeO}_6$  and  $\text{VO}_5$  units and the Th centers of adjacent chains

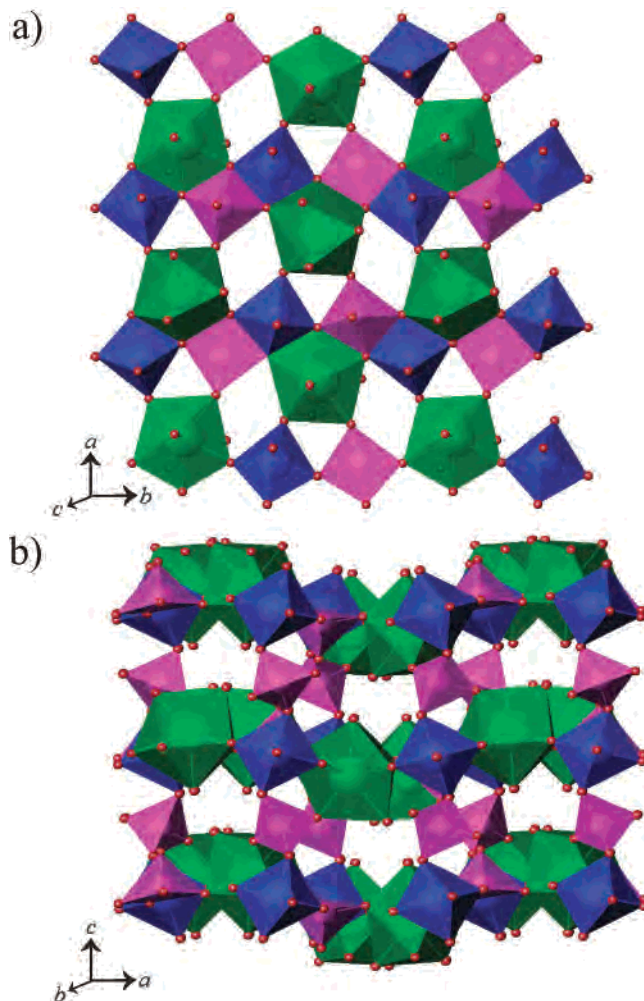


**Figure 4.** (a) A view of the  $\text{ThO}_9$ ,  $\text{VO}_5$ , and  $\text{TeO}_6$  units that form a continuum of edge-sharing interactions to yield Th–V–Te oxide chains that extend along the  $b$ -axis. Corner-sharing interactions between  $\text{TeO}_6$  and  $\text{VO}_5$  units and the Th centers of adjacent chains form two-dimensional sheets in the  $[ab]$  plane. (b) The three-dimensional network of  $\text{Th}(\text{VO}_2)_2(\text{TeO}_6)(\text{H}_2\text{O})_2$  is formed by the linkage of these sheets through the  $\text{VO}_4$  units. The  $\text{VO}_4$  tetrahedra bridge the Th and Te centers from one sheet to thorium and tellurium in an adjacent sheet in the  $c$  direction. Vanadium polyhedra are shown in magenta, thorium are in green, and tellurium are in blue.

lead to the formation of two-dimensional sheets in the  $[ab]$  plane. The three-dimensional network is formed by the linkage of these sheets through the  $\text{VO}_4$  units, as is shown in Figure 4b. The  $\text{VO}_4$  tetrahedra bridge the Th and Te centers from one sheet to thorium and tellurium in an adjacent sheet in the  $c$  direction.

**Optical Properties.** The optical properties of  $\text{Th}(\text{VO}_2)_2(\text{TeO}_6)(\text{H}_2\text{O})_2$  have been evaluated using UV–vis diffuse reflectance spectroscopy. This compound displays a weak absorption band near 387 nm that is followed by strong absorption feature at approximately 600 nm. The spectrum is similar that of other vanadyl oxoanion compounds such as  $\text{A}[\text{VO}_2(\text{IO}_3)_2]$  ( $\text{A} = \text{K}, \text{Rb}$ ) and  $\text{A}[(\text{VO}_2)_2(\text{IO}_3)_3\text{O}_2]$  ( $\text{A} = \text{NH}_4, \text{Rb}, \text{Cs}$ ).<sup>19</sup> It is likely that the visible absorption

(17) Brown, I. D.; Altermatt, D. *Acta Crystallogr.* **1985**, *B41*, 244.

(18) Brese, N. E.; O’Keeffe, M. *Acta Crystallogr.* **1991**, *B47*, 192.

(19) Sykora, R. E.; Ok, K. M.; Halasyamani, P. S.; Wells, D. M.; Albrecht-Schmitt, T. E. *Chem. Mater.* **2002**, *14*, 2741.

for  $\text{Th}(\text{VO}_2)_2(\text{TeO}_6)(\text{H}_2\text{O})_2$  can be attributed to charge transfer in the vanadyl units.

**Thermal Behavior.** Differential scanning calorimetry measurements on  $\text{Th}(\text{VO}_2)_2(\text{TeO}_6)(\text{H}_2\text{O})_2$  show that the compound is stable to approximately 250 °C; thereafter it begins to lose water with an endotherm centered at 282 °C. This is followed by further decomposition with three endotherms at 418, 456, and 472 °C followed by a small exotherm at 534 °C. TGA measurements show that the endotherm near 456 °C is associated with the loss of Te from the sample.  $\text{Th}(\text{VO}_2)_2(\text{TeO}_6)(\text{H}_2\text{O})_2$  decomposes primarily to  $\text{Th}(\text{VO}_3)_4$  when heated at 600 °C in air as determined by X-ray powder diffraction measurements.<sup>20</sup>

### Conclusions

The synthesis of the first actinide tellurate,  $\text{Th}(\text{VO}_2)_2(\text{TeO}_6)(\text{H}_2\text{O})_2$ , has been achieved via the hydrothermal

(20) Quarton, M.; Pages, M.; Freundlich, W. *C. R. Seances Acad. Sci., Ser. C* **1978**, 286, 369–71.

reaction of  $\text{Th}(\text{NO}_3)_4 \cdot x\text{H}_2\text{O}$  with  $\text{V}_2\text{O}_5$  and  $\text{H}_6\text{TeO}_6$ . The remarkably complex three-dimensional structure of  $\text{Th}(\text{VO}_2)_2(\text{TeO}_6)(\text{H}_2\text{O})_2$  is a direct consequence of the high coordination number of Th combined with the variable coordination of vanadium and the remarkable ability of tellurate to simultaneously bind seven metal centers. This first example of a thorium tellurate points to what is likely to be a large family of structurally diverse actinide tellurate compounds.

**Acknowledgment.** This work was supported by the Chemical Sciences, Geosciences and Biosciences Division, Office of Basic Energy Sciences, Office of Science, Heavy Elements Program, U.S. Department of Energy, under Grant DE-FG02-01ER15187.

**Supporting Information Available:** X-ray crystallographic file for  $\text{Th}(\text{VO}_2)_2(\text{TeO}_6)(\text{H}_2\text{O})_2$  in CIF format. This material is available free of charge via the Internet at <http://pubs.acs.org>.

IC048256J